Efficient White Organic Light-emitting Device by utilizing a Blue-emitter Doped with a Red Fluorescent Dopant

Jongtae Lim[a], Young-Joo Ahn[a], Gi-Wook Kang[a**], Namheon Lee[a**], Mun-Jae Lee[a**],

HeeYoung Kang[a***], Changhee Lee[a*],   Young Wook Ko[b], and Jin Ho Lee[b*]

Abstract

We synthesized bis (2-methyl-8-quinolinolato)(triphenylsiloxy) aluminum (III) (SAlq), a blue-emitting material having a high luminous efficiency, through a homogeneous-phase reaction. The photoluminescence (PL) and electroluminescence (EL) spectra of SAlq show two peaks at 454 nm and 477 nm. Efficient white light-emitting devices are fabricated by doping SAlq with a red fluorescent dye of 4-dicyanomethylene-2-methyl-6-{2-(2,3,6,7-tetrahydro-1H,5H-benzo[i,j]quinolizin-8-yl)vinyl}-4H-pyran (DCM2). The incomplete energy transfer from blue-emitting SAlq to red-emitting DCM2 results in light-emission of both blue and orange colors. Devices with the structure of ITO/TPD (50 nm)/SAlq:DCM2 (30 nm, 0.5 %)/Alq$_3$ (20 nm)/LiF (0.5 nm)/Al show EL peaks at 456 nm and 482 nm originating from SAlq and at 570 nm from DCM2, resulting in the Commission Internationale d'Eclairage (CIE) chromaticity coordinates of (0.32, 0.37). The device exhibits an external quantum efficiency of about 2.3 % and a luminous efficiency of about 2.4 lm/W at 100 cd/m^2. A maximum luminance of about 23,800 cd/m^2 is obtained at the bias voltage of 15 V.

1. Introduction

An organic light-emitting device (OLED) is one of the most promising next-generation large-area flat panel display systems since the introduction of efficient OLED utilizing this (8-quinolinolato-N^1, O^3) aluminum (III) (Alq3) [1] by Tang and van Slyke. A variety of materials have been reported for electrolu-minescence (EL) with various-color emission [2]. However, there are only few organic materials that can generate a white light-

emission [3].

White light-emission is very important when applying OLEDs to a full-color display, a backlight of LCDs, and solid-state lightings. J. Kido et al. and other researchers have reported various types of white OLEDs [3-9]. In general, multilayer structures of two complementary color emitting layers or RGB primary color emitting layers are normally used for white light-emitting devices [3].

White light-emission in doped devices is affected by the energy transfer from the host to the dopant as well as charge carrier trapping at dopant molecules. In addition, the low fluorescent efficiency of blue-emitting materials in such devices makes the Commission Internationale d'Eclairage (CIE) chromaticity coordinates deviate from a balanced white point of (0.333, 0.333). Therefore, efficient blue-emitting materials are essential for developing white light-emitting devices. However, blue emitting materials with high brightness and thermal stability still remain to be developed   [11].
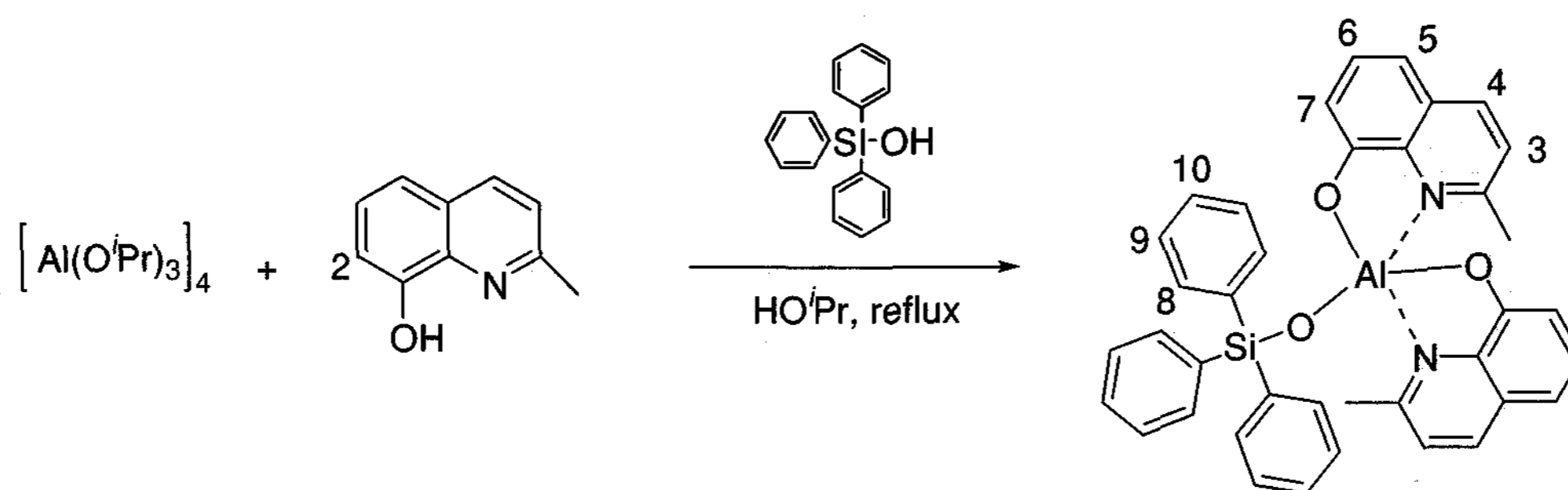
Fig. 1. Synthetic mechanism of bis(2-methyl-8-quinolinolato)(triphenylphenoxy)aluminum (III).

In this work, we report the synthesis of blue-emitting bis(2-methyl-8-quinolinolato) (triphenylsiloxy) aluminum (III), (SAlq) and the fabrication of efficient white organic light-emitting devices with the emitting layer of SAlq doped with 4-dicyanomethylene-2-methyl-6-{2-(2,3,6,7-tetrahydro-1H,5H-benzo[i,j]quinolizin-8-yl)vinyl}-4H-pyran (DCM2). It is noted that efficient white light emission can be achieved with a single emitting layer by doping a red fluorescent dopant into a blue-emitting host layer. Although it is quite difficult to avoid a significant amount of energy being transferred from the blue host to the red dopant in such structure, we find that the energy transfer from a blue-emitting SAlq to a red-emitting DCM2 is not completely transferred and therefore, result in both blue and red emission having similar relative intensities.

2. Experimental

2. 1 Synthesis of SAlq

SAlq was synthesized in high yield and high purity through the homogeneous-phase reaction between aluminium iso-propoxide and two ligand of 2-methyl-8-quinolinol and triphenylsilanol at reflux condition as shown in Fig. 1. All manipulations were performed under nitrogen atmosphere, and all solvents and chemicals were reagent grade. A three-necked flask (250 ml) containing a magnetic stir bar and fitted with a reflux condenser, a rubber septum, and gas inlet tube was charged with aluminum iso-propoxide (1.00 g, 4.90 m mol) and iso-propanol (100 ml) under nitrogen atmosphere. The slurry solution was heated for several minutes until the solid dissolved. The solution of iso-propanol containing 2-methyl-8-quinolinol (0.78 g, 4.90

m mol) was added to colorless solution, which formed, over a period of 0.5 hour under reflux condition using cannula, and stirred rapidly for 1 hour. The mixture of 2-methyl-8-quinolinol (0.78 g, 4.90 m mol) and triphenylsilanol (2.76 g, 9.80 m mol) dissolved in 50 ml of iso-propanol was added drop by drop, using cannula, over a period of 1 hour under reflux condition to the aluminum iso-propoxide solution. A white solid was precipitated immediately, but the solution was stirred for an additional 1 hour under reflux condition after all reactants had been added. The white precipitate was collected by filtration, washed with ca. 50 ml of hot iso-propanol, and then, two more times with ca. 50 ml of hot diethylether, Finally, they were allowed to dry under a reduced pressure to yield the white powder (2.50 g, 83 %, based on aluminum iso-propoxide).

The purity of SAlq was characterized by ^{1}H-NMR, ^{13}C-NMR, PL spectra, elemental analysis, and melting test. ^{1}H and ^{13}C-NMR spectra were recorded on Varian Unity-400 spectrometer with TMS as internal standard and elemental analysis was performed by EA-1110 (CE Instruments Co., Ltd.). The PL spectrum of SAlq thin film deposited onto quartz substrate was measured with a RF-5301PC spectrofluorophotometer (Shimazu Co., Ltd.). The absorption spectrum was measured with a Cary 500 UV-Vis spectrophotometer (Varian Co. Ltd.). The characterization results of SAlq can be summarized as follows: mp 248 ~ 249 °C; ^{1}H NMR (400.267 MHz, CDCl$_3$ δ in ppm): 8.11 (d, 2H, 4-H in quinoline, $^3J_{4,3}$= 8.4 Hz), 7.45 (t, 2H, 6-H in quinoline, $^3J_{6,5}$= 8.1 Hz, $^3J_{6,7}$= 7.6 Hz), 7.21 (d, 6H, 8-H in Ph, $^3J_{8,9}$= 7.5 Hz), 7.18 (d, 2H, 3-H in quinoline, $^3J_{3,4}$= 8.4Hz), 7.17 (d, 3H, 10-H in Ph, $^3J_{10,9}$= 7.2 Hz), 7.16 (d, 2H, 5-H in quinoline, $^3J_{5,6}$ =8.1 Hz), 7.08 (d, 2H, 7-H in quinoline, $^3J_{7,6}$= 7.6 Hz),

14

7.02 (t, 6H, 9-H in Ph, $^3J_{9,8}$= 7.5 Hz, $^3J_{9,10}$= 7.2 Hz), 2.61 (s, H, Me); ^{13}C NMR(400.267 MHz, CDCl$_3$ δ in ppm): 157.5, 156.3, 139.3, 138.7, 138.6, 134.7, 128.9, 128.6, 127.1, 124.1, 114.0, 112.5, 23.0; Anal. Calcd for C$_{38}$H$_{31}$O$_3$N$_3$AlSi: C, 73.76; H, 5.05; N, 4.53. Found: C, 73.61; H, 5.11; N, 4.49.

2. 2   Fabrication of electroluminescent devices

The device was fabricated by vacuum depositions of organic layers, LiF (0.5 nm), and Al electrode on top of indium tin oxide (ITO) substrates with a sheet resistance of about 10Ω/▯. The ITO coated glass substrate was cleaned by sonication in trichloroethane (TCE), iso-propanol, acetone and methyl alcohol, and rinsed in deionized water. The hole-transporting layer (HTL), N, N'-diphenyl-N,N'-di(3-methyl-phenyl)-1,1'-biphenyl-4, 4' -diamine (TPD) or 4,4'bis[N-(1-napthyl)-N-phenyl-amino]-biphenyl ((-NPD) having a thickness of 50 nm was deposited on to the ITO by thermal evaporation under a base pressure of 2x10^{-6} torr. On top of the TPD layer, SAlq and DCM2 were co-deposited with a thickness of 30 nm. The doping concentration of DCM2 in SAlq was about 0.5 %. A 30-nm-thick Alq$_3$ was deposited as an electron-transporting layer (ETL), followed by a 0.5-nm-LiF and Al electrode were deposited. The deposition rates and the thickness of the deposited layers were monitored by a thickness/rate controller.

The I-V-L characteristics were measured with a Keithley 236 source-measure unit. The intensity of the emission from the devices was simultaneously measured with a Keithley 2000 multimeter equipped with a calibrated Si photodiode or a photomultiplier tube (ARC P2 PMT) through an monochromator (ARC 275). The external EL quantum efficiency (QE), the ratio of the emitted photons to the injected charges, was calculated from the luminous output measured by the calibrated Si photodiode.

3. Results and Discussion

3.1   Synthesis of bis (2-methyl-8-quinolinolato) aluminum (III)

As shown in Fig. 1, bis (2-methyl-8-quinolino-lato)(triphenylsiloxy) aluminum (III) was easily synthe-sized from one-pot reaction through the homogeneous-phase reaction between aluminum iso-propoxide and two ligand of 2-methyl-8-quinolinol and triphenylsilanol under reflux condition. Bis (2-methyl-8-quinolinolato) (triphenylsiloxy) aluminum (III) was obtained at a high yield of 83 % under a reflux condition and was characterized from 1H-NMR spectrum as shown in Fig. 2, ^{13}C-NMR spectrum in Fig. 3, and an element analysis. The results show that there is one isomer exists.
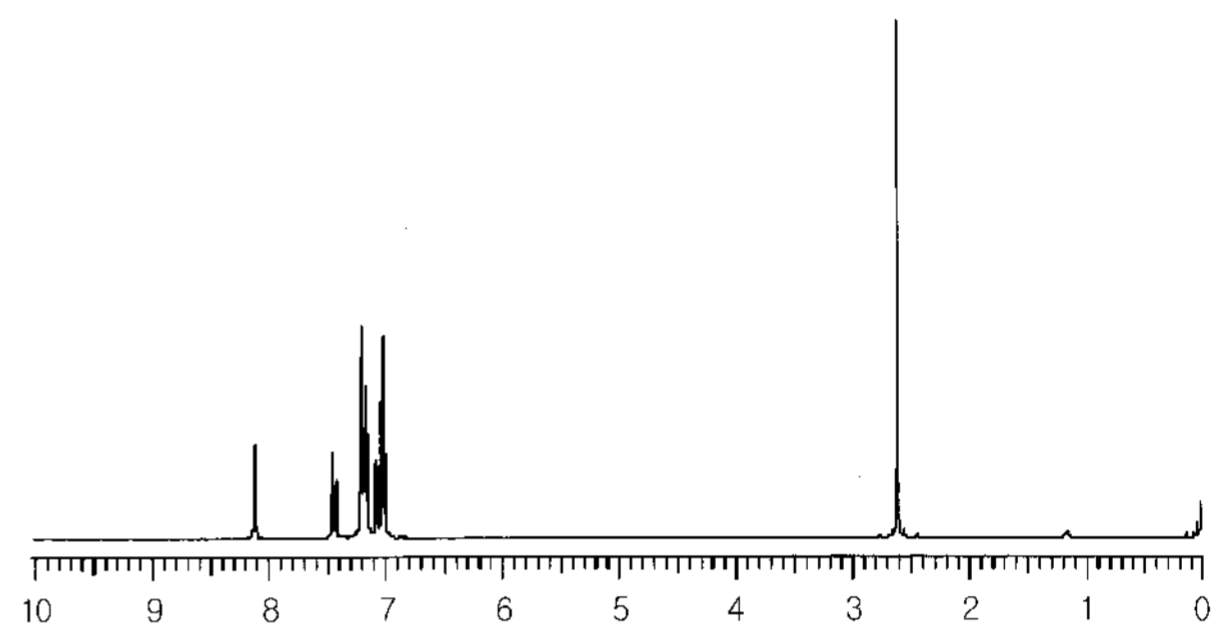

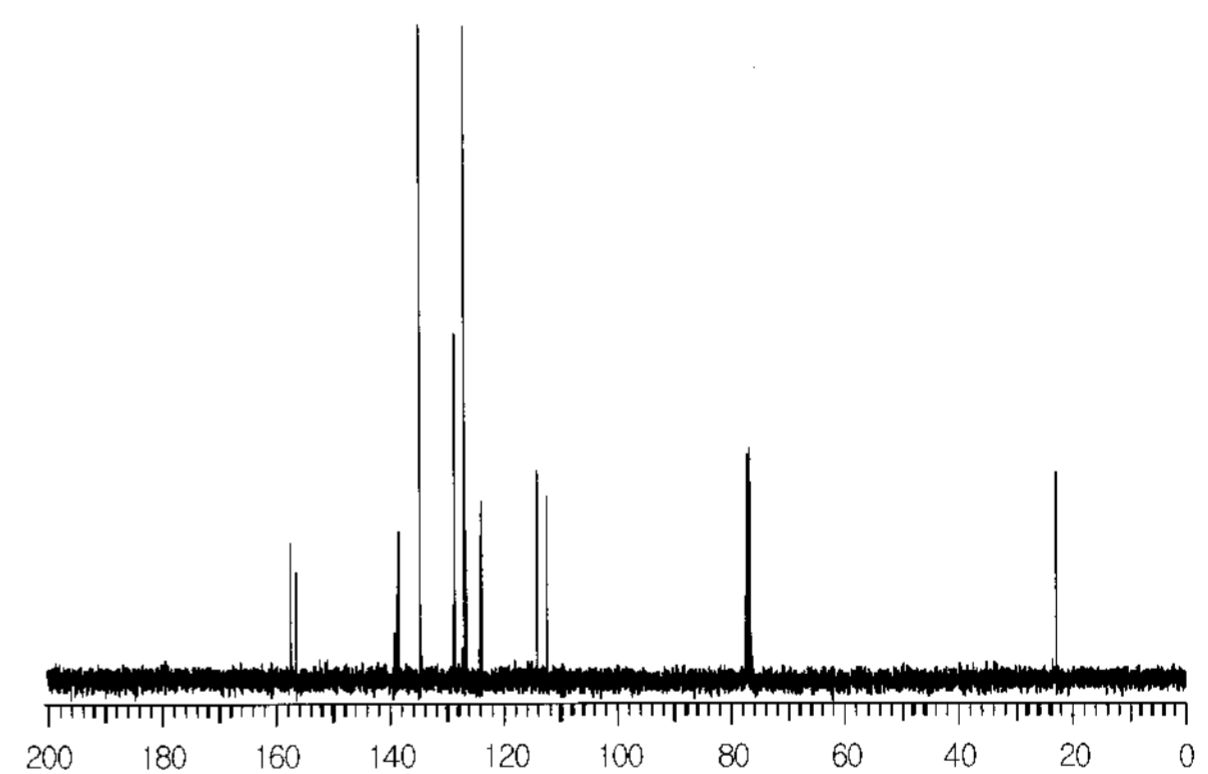**Fig. 2.** ^{1}H-NMR spectrum of bis (2-methyl-8-quinolinolato) (triphenylsiloxy) aluminum (III) in CDCl$_3$.

Fig. 3. ^{13}C-NMR spectrum of bis (2-methyl-8-quinolinolato) (triphenylsiloxy) aluminum (III) in CDCl$_3$.

To increase the stability of the aluminum complex, the metal coordination sphere was saturated by introducting of bulky substitution such as phenyl group on siloxy ligand. The electron-transporting ability of quinoline-complexes depends on overlapping among pyridyl rings [12]. The methyl substitutions on pyridyl part in quinoline enhance steric hindrance and decrease intermolecular interactions, and recrystallization, melting point, and glass-transition temperature [13]. Therefore, it is possible to increase the chemical and thermal stability

of the synthesized SAlq. Analysis of the residues through 1H-NMR spectrum, after remelting, shows that it does not decompose even after repeating three times. In general, thermally induced degradation is due to morphological instability of amorphous organic films. The crystallization or aggregation by an intermolecular interaction is a typical form of instability among organic films. Therefore, the increased thermal stability among SAlq indirectly that the implies device is more stable.

3.2 Absorption, photoluminescence excitation, and photoluminescence spectra of SAlq

Fig. 4 (a) exhibits the optical absorption spectrum of SAlq measured at wavelengths between (=200 and 450 nm. It shows peaks at 362 nm and 262 nm in solid films. The transition band at 262 nm is the 1Bb transition that is also found in the solution spectrum of Alq3 [14]. The optical transition responsible for photoluminescence (PL) in bis (8-quinolinolato)(aryloxy) aluminum (III) complexes (aryloxy=triphenylsiloxy or phenoxy derivatives) depend more on 8-quinolinolato ligands than siloxy ligand. This transition is due to a $\pi \rightarrow \pi^*$ charge transfer from the electron rich phenoxide ring (location of the highest occupied molecular orbital, or HOMO) to the electron deficient pyridyl ring (location of the lowest unoccupied molecular orbital, or LUMO) [15]. Therefore, as reported previously [16], the substitution of an electron-donating group on pyridyl ring raises the energy of the LUMO. The methyl substituents in pyridyl part on 8-quinolinolato ligand increase the energy band gap, causing in a hypsochromic shift to occur.
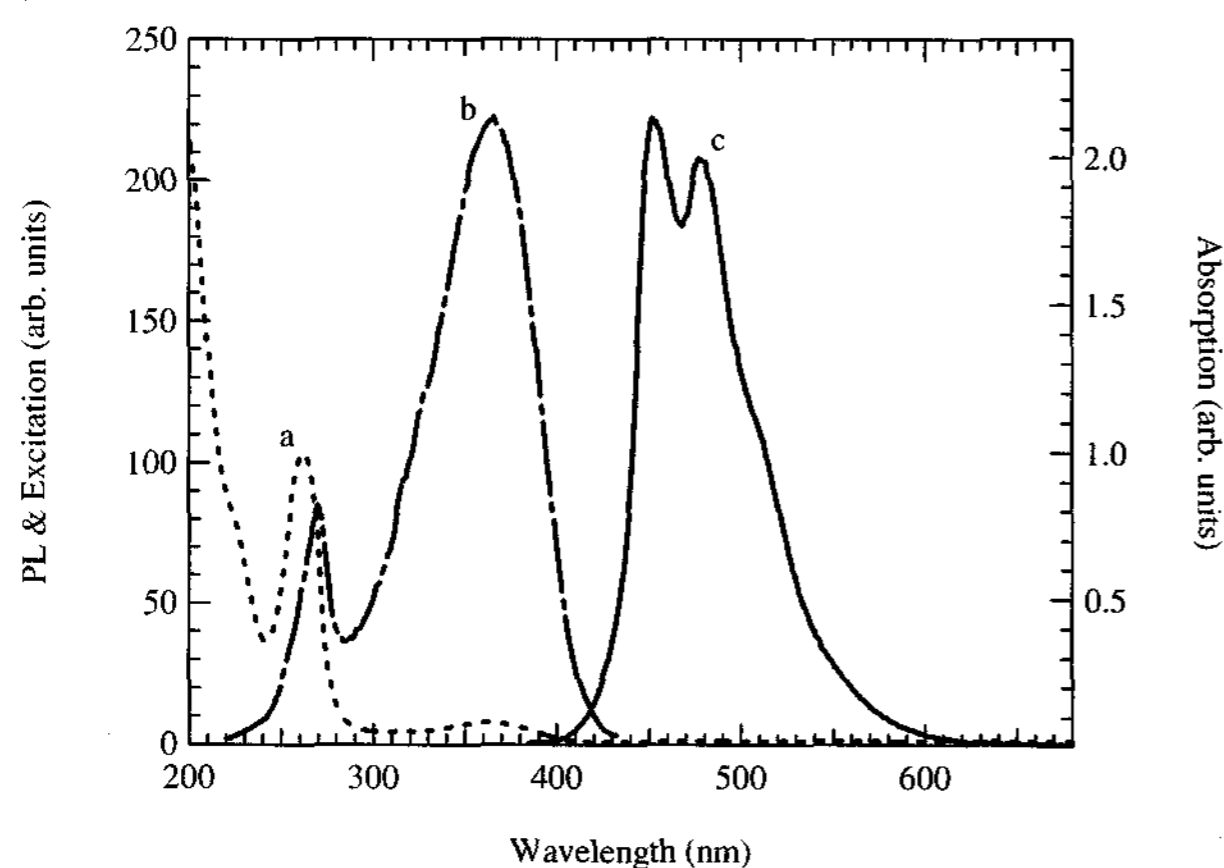

Fig. 4. (a) Optical absorption spectrum, (b) photoluminescence excitation spectrum, and (c) PL spectrum of SAlq film.

Figs. 4 (b) and (c) show the PL excitation (PLE) and PL spectra of SAlq deposited with the thickness of 100 nm on quartz substrates. The PLE spectrum shows two peaks of 270 and 365 nm at emission wavelengths of 452 nm. The PL spectrum shows two peaks of 454 nm and 477 nm and a shoulder around 510 nm at excitation wavelength of 365 nm.
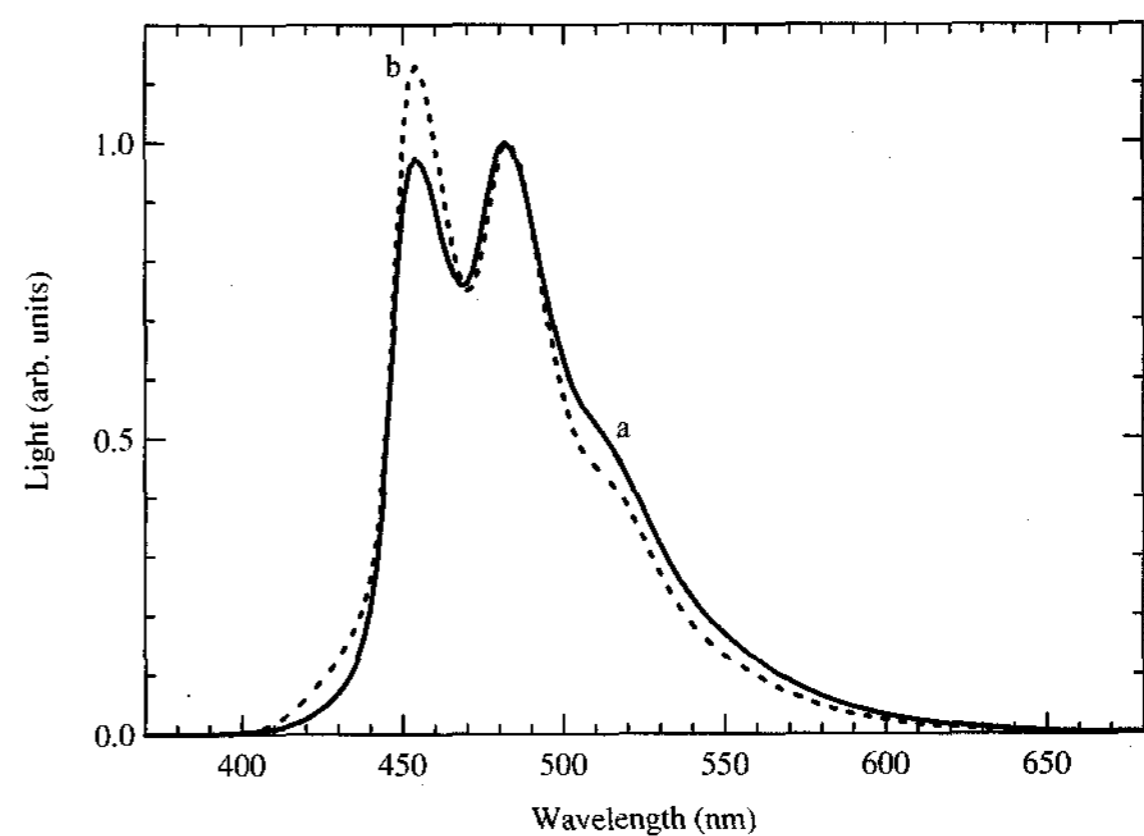

Fig. 5. Electroluminescence spectra for (a) ITO/TPD (50 nm)/SAlq (30 nm)/Alq3 (20 nm)/LiF (0.5 nm)/Al and (b) ITO/(-NPD (50 nm)/SAlq (30 nm)/Alq3 (20 nm)/LiF (0.5 nm)/Al.
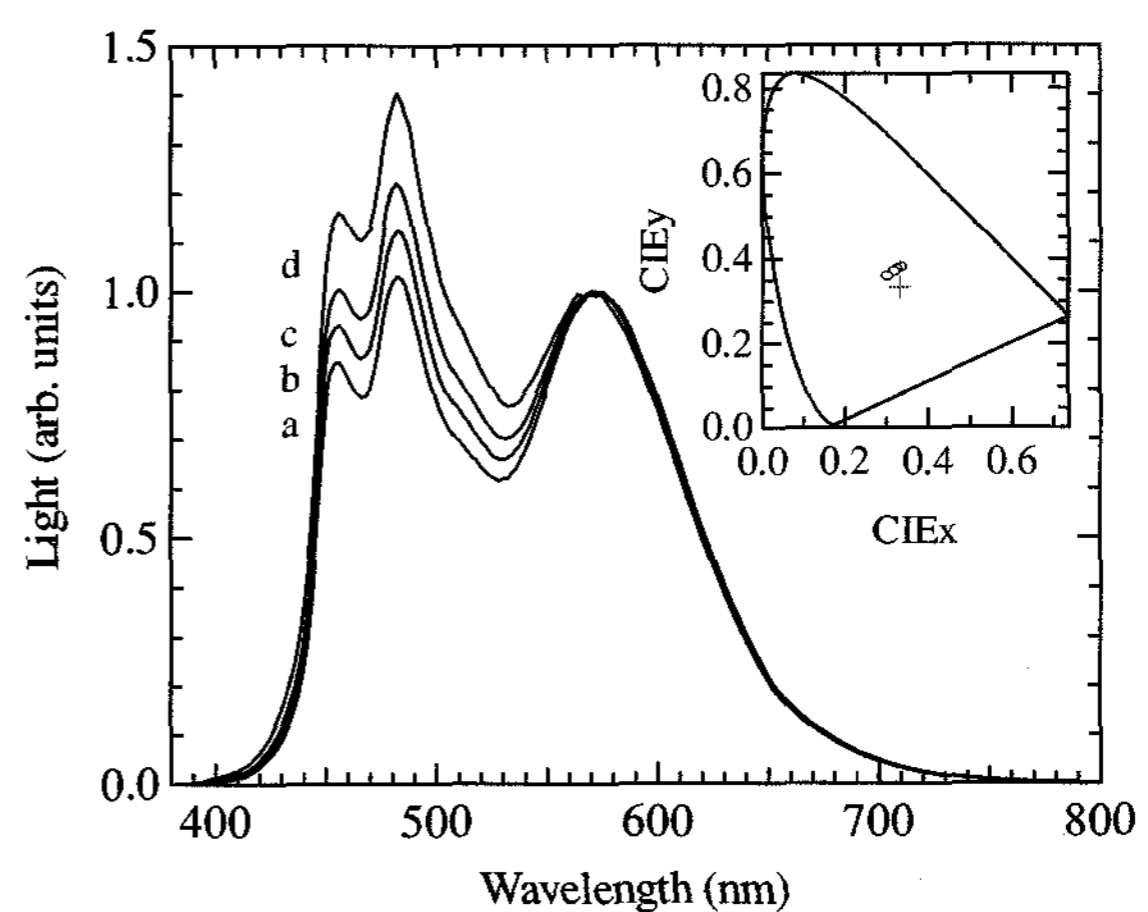

Fig. 6. Variation of the EL spectra with the current density for ITO/TPD (50 nm)/SAlq:DCM2 (0.5 %, 30 nm)/Alq3 (20 nm)/LiF (0.5 m)/Al at 17 (a), 35 (b), 70 (c), and 174 mA/cm² (d). Inset: the CIE chromaticity diagram for the corresponding EL spectra.

Fig. 5 shows the EL spectra of SAlq with different HTL of TPD or (-NPD, ITO/TPD (50 nm)/SAlq (30 nm)/Alq3 (20 nm)/LiF (0.5 nm)/Al (a) or ITO/(-NPD (50

nm)/SAlq (30 nm)/Alq3 (20 nm)/LiF (0.5 nm)/Al (b). Both devices exhibit almost identical EL spectra with two peaks at 454 nm and 482 nm and a shoulder around 510 nm. In addition, the EL spectra are very similar with the PL spectrum of SAlq. Therefore the blue EL emission originates from SAlq, and not from the blue-emitting HTL such as TPD or (-NPD. The device shown in Fig. 5 (a) demonstrates a maximum quantum efficiency (QE) of about 3.0 % and a luminous efficiency of about 2.5 lm/W.

A white light-emitting device was fabricated by doping small concentration (0.5 %) of DCM2 into SAlq layer. The device structure was ITO/TPD (50 nm)/SAlq:DCM2 (30 nm, 0.5 %)/Alq3 (20 nm)/LiF (0.5 nm)/Al. Fig. 6 shows the variation of the EL spectra when the current density is changed from 17 to 174 mA/cm^2. The inset shows the CIE chromaticity diagram for the corresponding EL spectra. It can be seen that the device exhibits EL peaks at both SAlq and DCM2. Therefore, the incomplete energy transfer from SAlq to DCM2 creates possibility of producing white light-emission by tuning the relative EL intensities of SAlq and DCM2. By adjusting the DCM2 concentration and the thickness of DCM2 doped SAlq layer, we can obtain a balanced white light emission for the device with the DCM2 concentration of about 0.5 % and the SAlq:DCM2 thickness of about 30 nm. As the current density increases, the blue part of the EL spectra shown in Fig. 6 increases slightly and the CIE coordinates changes from (0.34, 0.38) at a current density of 17 mA/cm^2 to (0.30, 0.36) at 174 mA/cm^2. However, the change in the CIE coordinates with the current density is relatively small compared with the devices of multiple light-emitting layers which suffer a color change with the bias voltage due to the movement of carrier recombination zone and exciton distribution over multiple light-emitting layers. Therefore, the relatively stable color coordinates under the variation of the current density is a positive feature of the device with a single light-emitting layer of SAlq:DCM2

Fig. 7 shows the current-voltage-luminescence (I-V-L) characteristics of ITO/TPD (50 nm)/SAlq:DCM2 (30 nm, 0.5 %)/Alq3 (20 nm)/LiF (0.5 nm)/Al. The onset voltage of the light emission is about 3 V. The maximum luminance of 23,800 cd/m^2 was achieved at 15 V and 782 mA/cm^2.

Fig. 8 shows the external quantum efficiency (QE) and the power efficiency for the same device as a function of the current density. The device shows an external QE of about 2.3 % and a luminous efficiency of 2.4 lm/W at a luminance of 100 cd/m^2 (bias voltage of 7 V and current density of 1.9 mA/cm^2).
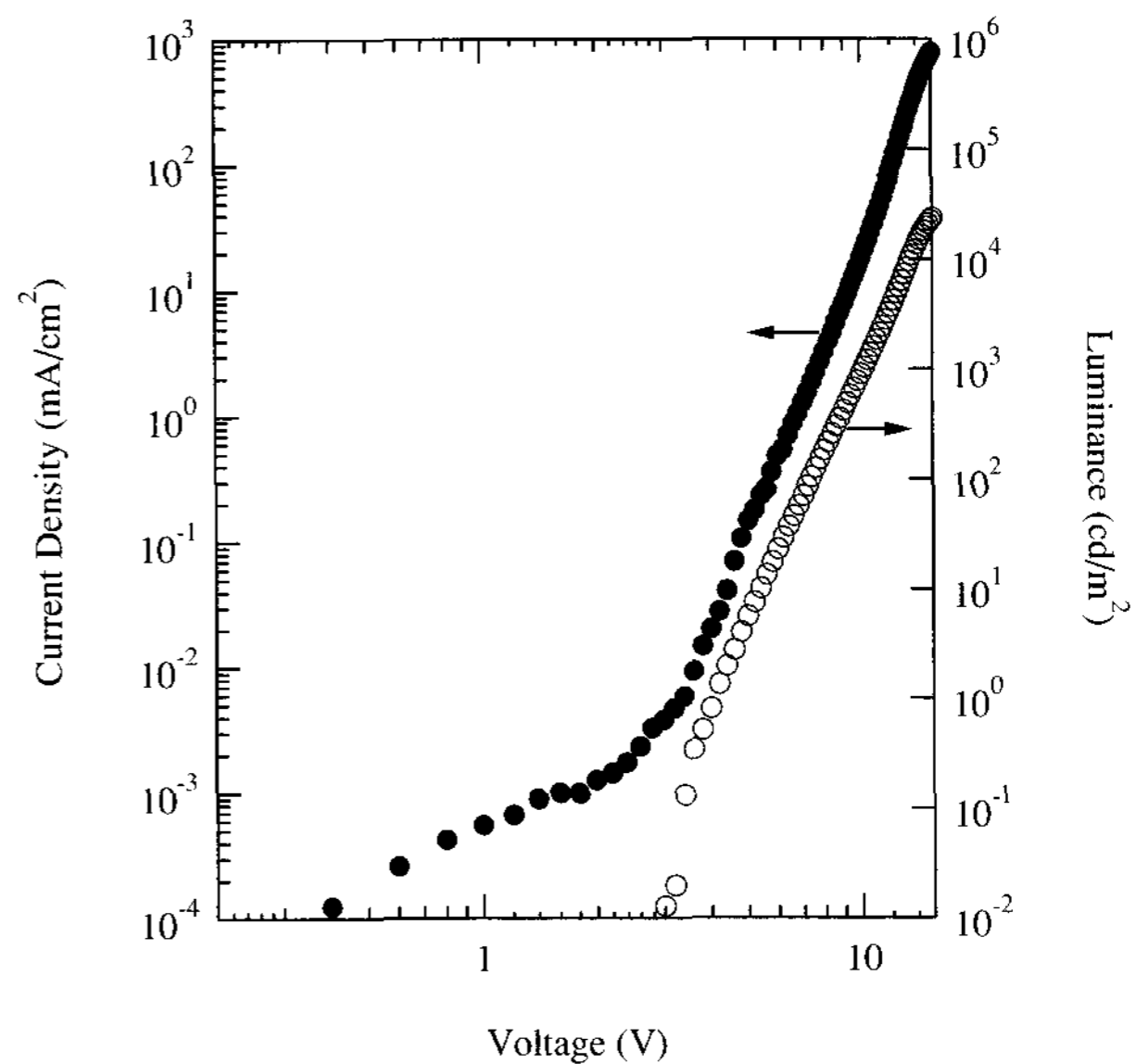

Fig. 7. The current-voltage-luminescence characteristics of ITO /TPD (50 nm)/SAlq:DCM2 (30 nm, 0.5 %)/Alq$_3$ (20 nm)/LiF (0.5 m)/Al.
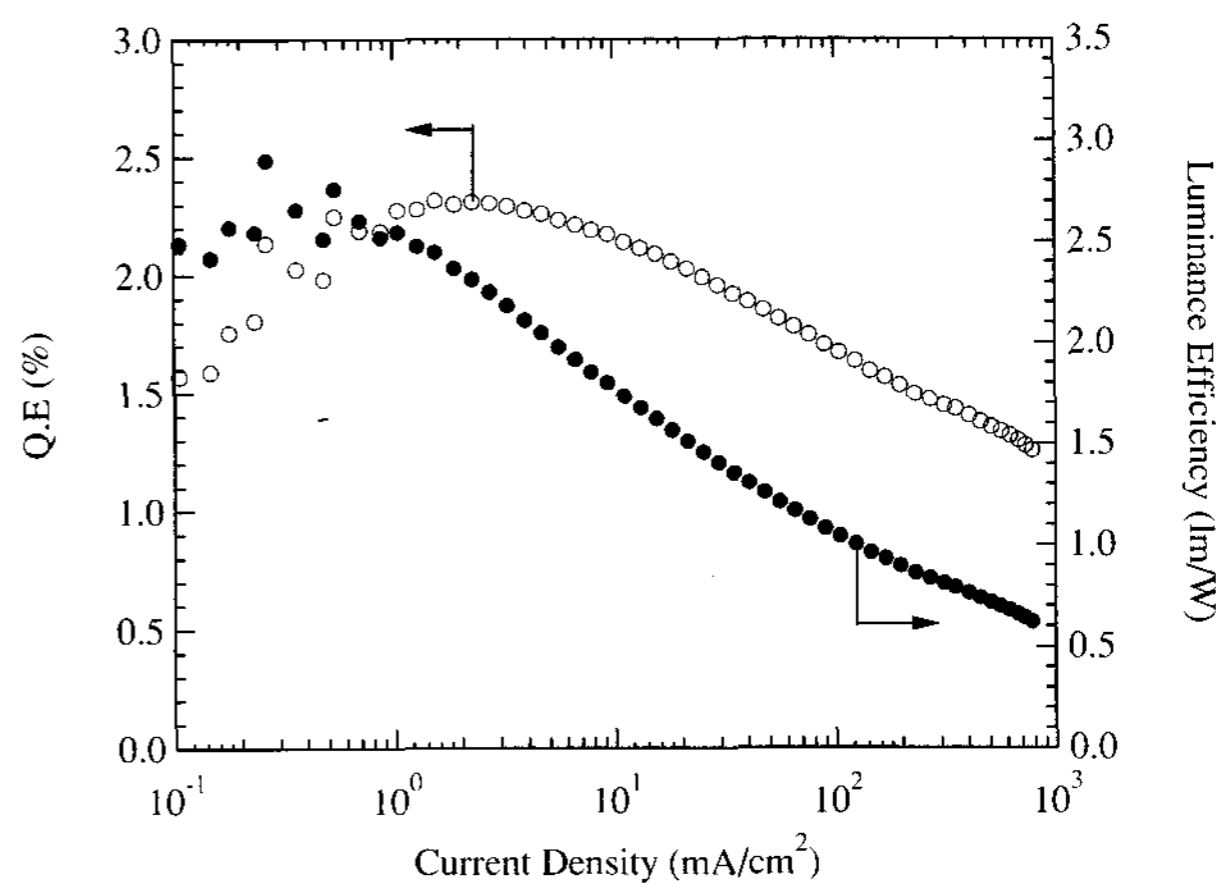

Fig. 8. The external quantum efficiency and the power efficiency as a function of the current density for ITO/TPD (50 nm)/SAlq:DCM2 (30 nm, 0.5%)/Alq$_3$ (20 nm)/LiF (0.5 nm)/Al.

4. Conclusions

Bis(2-methyl-8-quinolinolato) (triphenylsiloxy) aluminum (III) (SAlq) was synthesized at high purity and high yield through a homogeneous one-pot reaction. The blue device, where a SAlq was used as an active layer,

showed an external quantum efficiency of about 3.0 % and a luminous efficiency of about 2.5 lm/W. By doping DCM2 into Salq, we were able to fabricate an efficient white light-emitting device with a single emitting layer. The device with the structure of ITO/ TPD (50 nm)/SAlq:DCM2 (0.5 %, 30 nm)/Alq3 (20 nm)/LiF (0.5 nm)/Al exhibited white EL emission with an external QE of about 2.3 %, a luminous efficiency of about 2.4 lm/W, and the CIE chromaticity coordinates of (0.32, 0.37) at the luminance of 100 cd/m^2. The maximum luminance of 23,800 cd/m^2 was achieved at 15 V and 782 mA/cm^2.

References

[1] C. W. Tang and S. A. VanSlyke, Appl. Phys. Lett. **51**, 913 (1987).

[2] U. Mitschke and P. Bauerle, J. Mater. Chem. **10**, 1471 (2000).

[3] J. Kido, "Organic Electroluminescent Materials and Devices", Ed., S. Miyata and H. S. Nalwa (Gordon and Breach Science Publishers, Amsterdam, 1997), p. 335.

[4] Y. Hamada, T. Sano, M. Fujita, T. Fujii, Y. Nishino, and K. Shibata, Jpn. J. Appl. Phys. **32**, L917 (1993).

[5] S. Tokito, J. Takata, and Y. Taga, J. Appl. Phys. **77**, 1985 (1995).

[6] J. Kido, M. Kimura, and K. Nagai, Science **267**, 1332 (1995).

[7] K. Strukeji, R. H. Jordan, and A. Dodabalapur, J. Am. Chem. Soc. **118**, 1213 (1996).

[8] M. Granstom and O. Inganas, Appl. Phys. Lett. **68**, 147 (1996).

[9] R. S. Deshpande, V. Bulovic, and S. R. Forrest, Appl. Phys. Lett. **75**, 888 (1999).

[10] C.-H. Kim and J. Shinar, Appl. Phys. Lett. **80**, 2201 (2002).

[11] T. Noda, H. Ogawa, and Y. Shirota, Adv. Mater. **4**, 283 (1999).

[12] M. Sugimoto and S. Sakaki, J. Appl. Phys. **90**, 6092 (2001).

[13] L. S. Sapochak, A. Padmaperuma, N. Washton, F. Endrino, G. T. Schmett, J. Marshall, D. Fogarty, P. E. Burrows, and S. R. Forrest, J. Am. Chem. Soc. **123**, 6300 (2001).

[14] D.Z.Garbuzov, V. Bulovic, P.E. Burrows, and S. R. Forrest, Chem. Phy. Lett. **249**, 433 (1996).

[15] C. H. Chen and J. Shi, J. Coord. Chem. Rev. **171**, 161 (1998).

[16] A. Curioni, M. Boero and W. Andreoni, Chem. Phys. Lett. **294**, 263 (1998).